4　ROCK阻害剤

前述の通り，霊長類ES/iPS細胞を単一細胞にしてしまうとアポトーシスを起こして死滅してしまうため，細胞間接着を保ったままあらゆる操作を行わなければならない。そのため，熟練された技術が必要であり，研究発展の大きな障害となっていた。しかし近年，Rho結合リン酸化酵素（Rho-associated protein kinase：ROCK）に対する特異的阻害剤であるY-27632やHA-1077が単一細胞状態のヒトES細胞の生存を飛躍的に向上させることが示された[18]。ROCKは，低分子量GTP結合タンパク質のひとつであるRhoにより活性化を受けるリン酸化酵素であり，ROCKによるシグナル伝達は細胞の形態，収縮，遊走，増殖から分化誘導や細胞死に至るまでの多彩な細胞応答に関わることが知られている。この報告では，ヒトES細胞を単一細胞にして培養するとほとんどがアポトーシスにより死滅するが，ROCK阻害剤を培地に添加すると，アルカリホスファターゼ陽性コロニーが多数形成されることが示された。また，これらの細胞は*in vitro*における3胚葉系譜細胞に分化することが可能であり，さらに免疫不全マウスに移植すると，テラトーマが形成されることから分化万能性を維持していることも確認された[18]。すなわち，培地にROCK阻害剤を添加するという簡便な方法により，未分化状態・分化万能性を維持したままES/iPS細胞の単一細胞状態での操作が可能になった。その結果，これまで困難であった霊長類ES/iPS細胞への遺伝子導入，FACSによるソーティング後の維持[22]，さらにはiPS細胞の樹立時にも有用であることから[23]，現在ROCK阻害剤は様々な施設で広く用いられている。

5　ROCK阻害剤を用いた霊長類ES/iPS細胞の凍結保存

ROCK阻害剤を用いると，ヒトES細胞を単一細胞状態で効率的に凍結保存することが可能であるという報告がある[24,25]。筆者らも緩慢凍結法においては他の細胞株と同じように単一細胞の方がより効果的に凍結保存できるのではないかと考え，ヒトiPS細胞を凍結前または解凍・播種後にY-27632を含む培地で培養をするという条件の下，開発品を用いてヒトiPS細胞を凍結し，解凍後の回復率を検討した。

セミコンフルエント状態のヒトiPS細胞を，凍結する1時間前にY-27632を添加した培地で培養した。その後トリプシンにより培養容器から剥離し単一細胞にした後，開発品を用いて緩慢凍結法で凍結保存した。最適条件で解凍し，Y-27632を添加した培地で16時間培養した（表1）。その

表1　Y-27632の培地への添加条件

凍結前	解凍後	
−	−	(−/−)
+	−	(+/−)
−	+	(−/+)
+	+	(+/+)

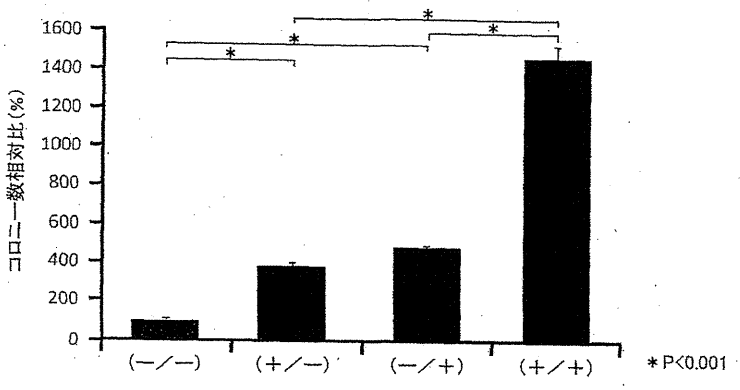

図3　凍結前・解凍後におけるY-27632の効果

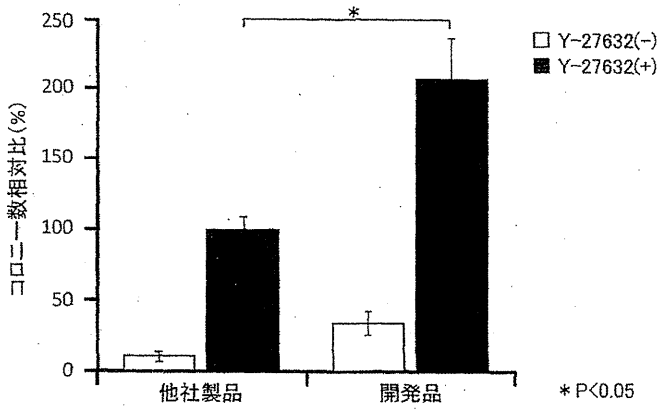

図4　他社製品との比較

後は通常の培地で培養し，培養8日目にアルカリホスファターゼ染色を行い，未分化状態のコロニー数を測定した。

その結果，Y-27632未添加の条件と比較し，細胞を凍結する前にY-27632を添加した培地で培養することで約4倍，細胞を解凍した後にY-27632を添加した培地で培養することで約5倍コロニー数が多いことが示された。さらに凍結前・解凍後どちらの培地にも添加すると約15倍と劇的にコロニー数が増加した（図3）。

また，市販の凍結保存液を用いて開発品との性能比較を行った。その結果，解凍後の培地にY-27632を添加した場合，開発品は市販の凍結保存液と比較し，約2倍コロニー数が多いことが確認された（図4）。この結果は，開発品の凍結保存能が他社製品より優れていることを示している。したがって，Y-27632と開発品を組み合わせて使用することにより操作が簡便になりかつ高効率

にヒトiPS細胞を凍結保存できることが示された。

6　再生医療実現のために

ヒトES/iPS細胞を用いた再生医療への期待が高まっているが，ヒトES/iPS細胞の樹立・維持の際に，ヒト以外の動物成分を含む試薬や培地を用いることは移植細胞の免疫拒絶の可能性や未知の病原体による感染の危険性がある。例えば，シアル酸は糖鎖の構成成分であるが，ウシ血清を含む培地で培養すると，細胞はウシ血清に含まれている異種成分由来のシアル酸であるN-グリコリルノイラミン酸（Neu5Gc）を取り込み，自身の糖鎖を合成してしまう。このような細胞を用いて移植に使用すると，Neu5Gcに対する抗体が産生されることが知られており[26]，免疫原性になる可能性がある。そのため，医療応用のためのES/iPS細胞の樹立，維持は可能な限り異種成分を除いた条件下で取り扱うことが望ましい。開発品には異種成分が含まれておらず，既知成分のみ配合されているため医療応用に適している。また，現在国内において，再生医療実現のため様々なヒトES/iPS細胞を大量に貯蔵する「細胞バンク」の整備が進められようとしている。そのためには凍結保存液は不可欠である。開発品は，細胞の凍結・解凍・輸送が簡便であり，大量処理が必要な細胞バンクにも有用であると期待している。

7　今後に向けて

霊長類ES/iPS細胞の凍結保存は研究者を満足させるようなレベルには達しておらず，開発途上の技術であるといっても過言ではない。特に解凍後の回復率はまだ低く，改善の余地が多く残されている。今後の基礎研究や再生医療の発展のためには，より回復率が高い凍結保存液を開発することが必要であると考えている。

文　献

1) C. Polge *et al.*, *Nature*, **164**, 666-666 (1949)
2) C. Polge and J. E. lovelock, *Vet. Rec.*, **64**, 396-397 (1952)
3) M. J. Ashwood-Smith and J. F. Loutit, *Blood*, **23**, 494-501 (1964)
4) D. E. Pegg, J. appl. *Phisiol.*, **19**, 123-126 (1964)
5) D. G. Whittingham *et al.*, *Science*, **187**, 411-414 (1972)
6) J. R. Dobrinsky, *Theriogenology*, **45**, 17-26 (1996)
7) W. F. Rall and G. M. Fahy, *Nature*, **313**, 573-575 (1985)
8) G. Vajta *et al.*, *Cryo-Letters*, **18**, 191-195 (1997)

9) G. Vajta *et al.*, *Mol. Reprod. Dev.*, **51**, 53-58 (1998)
10) G. Vajta *et al.*, *Acta Vet. Scand.*, **38**, 349-352 (1997)
11) M. J. Evans and M. H. Kaufman, *Nature*, **292**, 154-156 (1981)
12) 田川陽一ほか, 細胞工学, **14**, 946-955 (1995)
13) J. A. Thomson *et al.*, *Proc. Natl. Acad. Sci. U. S. A*, **92**, 7844-7848 (1995)
14) J. A. Thomson *et al.*, *Science*, **282**, 1145-1147 (1998)
15) K. Takahashi *et al.*, *Cell*, **131**, 861-872 (2007)
16) J. Yu and J. A. Thomson, *Genes Dev.*, **22**, 1987-1997 (2008)
17) H. Suemori *et al.*, *Dev. Dyn.*, **222**, 273-279 (2001)
18) K. Watanabe *et al.*, *Nat. Biotechnol.*, **25**, 681-686 (2007)
19) T. Fujioka *et al.*, *Int. J. Dev. Biol.*, **48**, 1149-1154 (2004)
20) B. E. Reubinoff *et al.*, *Hum. Reprod.*, **16**(10), 2187-2194 (2001)
21) M. Richards *et al.*, *Stem Cells*, **22**, 779-789 (2004)
22) N. Emre *et al.*, *PLoS ONE*, **5**, e12148 (2010)
23) I. Park *et al.*, *Nature*, **451**, 141-146 (2008)
24) X. Li *et al.*, *Hum. Reprod.*, **24**, 580-589 (2009)
25) H. Baharvand *et al.*, *Nat. Protoc.*, **5**(3), 588-594 (2010)
26) D. Ghaderi *et al.*, *Nat. Biotechnol.*, **28**(8), 863-867 (2010)

International Immunology Advance Access published March 15, 2014

International Immunology
doi:10.1093/intimm/dxu040

Activation-induced cytidine deaminase is dispensable for virus-mediated liver and skin tumor development in mouse models

Tung Nguyen[1], Jianliang Xu[1], Shunsuke Chikuma[1], Hiroshi Hiai[2], Kazuo Kinoshita[3], Kyoji Moriya[4], Kazuhiko Koike[5], Gian Paolo Marcuzzi[6], Herbert Pfister[6], Tasuku Honjo[1] and **Maki Kobayashi[1]**

[1]Department of Immunology and Genomic Medicine, Graduate School of Medicine, Kyoto University, Kyoto 606-8501, Japan
[2]Medical Innovation Center, Graduate School of Medicine, Kyoto University, Kyoto 606-8501, Japan
[3]Shiga Medical Center Research Institute, Moriyama, Shiga 524-8524, Japan
[4]Department of Infection Control and Prevention, University of Tokyo, Bunkyo, Tokyo 113-8655, Japan
[5]Department of Gastroenterology, University of Tokyo, Bunkyo, Tokyo 113-8655, Japan
[6]Institute of Virology and Center for Molecular Medicine Cologne, University of Cologne, Cologne D-50931, Germany

Correspondence to: T. Honjo; E-mail: honjo@mfour.med.kyoto-u.ac.jp

Received 26 December 2013, *accepted* 10 February 2014

Abstract

Activation-induced cytidine deaminase (AID) not only promotes immune diversity by initiating somatic hypermutation and class switch recombination in immunoglobulin genes but also provokes genomic instability by introducing translocations and mutations into non-immunoglobulin genes. To test whether AID is essential for virus-induced tumor development, we used two transgenic tumor models: mice expressing hepatitis C virus (HCV) core proteins (HCV-Tg), driven by the hepatitis B virus promoter, and mice expressing human papillomavirus type 8 proteins (HPV8-Tg), driven by the Keratin 14 promoter. Both strains were analyzed in the absence and presence of AID by crossing each with *AID*$^{-/-}$ mice. There was no difference in the liver tumor frequency between the HCV-Tg/*AID*$^{+/+}$ and HCV-Tg/*AID*$^{-/-}$ mice at 20 months of age although the *AID*$^{+/+}$ mice showed more severe histological findings and increased cytokine expression. Furthermore, a low level of AID transcript was detected in the HCV-Tg/*AID*$^{+/+}$ liver tissue that was not derived from hepatocytes themselves but from intra-hepatic immune cells. Although AID may not be the direct cause of HCV-induced oncogenesis, AID expressed in B cells, not in hepatocytes, may prolong steatosis and cause increased lymphocyte infiltration into HCV core protein-induced liver lesions. Similarly, there was no difference in the time course of skin tumor development between the HPV8-Tg/*AID*$^{-/-}$ and HPV8-Tg/*AID*$^{+/+}$ groups. In conclusion, AID does not appear to be required for tumor development in the two virus-induced tumor mouse models tested although AID expressed in infiltrating B cells may promote inflammatory reactions in HCV core protein-induced liver pathogenesis.

Keywords: hepatitis C virus, human papillomavirus type 8

Introduction

Activation-induced cytidine deaminase (AID) is essential for inducing DNA breaks during the somatic hypermutation and class switch recombination of immunoglobulin genes required for generating antibody diversity in activated B cells (1). AID generates physiological mutations during deliberate antibody development, but can also cause chromosomal translocations and mutations in proto-oncogenes when expressed aberrantly (2). Transgenic, ubiquitous over-expression of AID causes T-cell lymphoma and micro-adenoma in the lung (3) along with mutations in the TCR and c-myc genes. Chronic infections with micro-organisms such as helicobacter pylori (4), hepatitis C virus (HCV) (5–7), and human T-cell leukemia virus type 1 (8) induce the aberrant AID expression, which has been proposed to cause tumors by introducing translocations and somatic mutations into proto-oncogenes. In addition, AID expression is associated with chronic infections of these pathogens in human cases, in which it has also been proposed to contribute to tumor formation at least in part (4, 9). However, it has not been directly determined if virus- or bacteria-induced oncogenesis requires the action of AID.

Hepatocellular carcinoma (HCC) is the fifth most frequent cancer, and hepatitis B virus (HBV) and HCV infections are

the major risk factors for developing this cancer worldwide (10). In fact the risk of developing HCC is increased 11.5- to 17-fold in HCV-infected patients; however, antiviral therapies have limited effectiveness in only a small fraction of patients. Thus, elucidation of the mechanism(s) involved in promoting liver tumorigenesis is urgently required for developing a prevention strategy. As natural infection of HCV is restricted to humans and chimpanzees, several transgenic mouse models harboring parts of the HCV polyprotein have been generated to recapitulate HCC development (11). HCV, a small RNA virus, belongs to the Flaviviridae family and contains a 9.6-kb single-stranded RNA genome. The polyprotein encoded by the HCV genome is processed into the structural proteins (including core, E1 and E2) and the non-structural (NS) proteins (NS2-NS5) required for RNA genome replication by host and viral proteases (11). Among them, the HCV core protein has unique, multifunctional roles in apoptosis, signal transduction, reactive oxygen species formation, transformation and immune modulation (such as the up-regulation of TGF-β) (10) by interacting with many cellular proteins. Out of the 14 lines of HCV-transgenic mice developed, 5 HCV core protein-containing transgenic lines and 1 non-structural (NS5A) transgenic line can give rise to HCC, after the development of severe steatosis, a characteristic pathology associated with HCV infection (11–13). Especially, a transgenic mouse model expressing HCV core protein (HCV-Tg) driven HBV regulatory elements (12), which limits HCV core protein expression strictly in hepatocytes, had the highest HCC prevalence among many HCV protein transgenic model mice (11, 13); therefore, this model mouse line seemed to be a good tool to investigate AID expression in hepatocytes and its contribution to the mechanism of HCC development.

On the other hand, the human papillomavirus (HPV) family of small DNA tumor viruses, of which there are over 120 types, can cause hyper-proliferative lesions in cutaneous and mucosal epithelia (14). Among them, HPV5 and HPV8 are classified as high-risk beta-type papilloma viruses and are the two major causes of cutaneous squamous cell carcinoma (SCC) in epidermodysplasia verruciformis patients. The development of SCC by HPV8 is promoted by a series of carcinogenic events, including DNA damage, evasion of apoptosis, mutation mediated by E6 protein and enhanced proliferation after ultraviolet light B exposure, mediated by E7 protein (14). Unlike HCV infection, HPV8 does not cause severe inflammation; however, DNA damage is an important carcinogenic process associated with this virus. A transgenic mouse model in which HPV8 early genes are expressed under the control of the Keratin 14 (K14) promoter (15) exhibits significant papilloma development (up to 91% of the HPV8-Tg mice) and malignant progression (6% of the HPV8-Tg mice backcrossed to FVB/N).

To determine whether AID is aberrantly induced by HCV or HPV8 and required for virally induced tumorigenesis, we crossed HCV-Tg or HPV8-Tg mice with *AID*$^{-/-}$ mice and compared the tumorigenesis frequencies in the *AID*$^{+/+}$ and *AID*$^{-/-}$ mice. We also examined the AID expression levels in the affected tissues. We found that HCV-Tg mice exhibited enhanced AID expression in the B cells infiltrating the liver, and that the steatosis and lymphocytic follicle formation were more severe in the HCV-Tg/*AID*$^{+/+}$ than in the HCV-Tg/*AID*$^{-/-}$ mice. However, the HCC prevalence at 20 months of age was not remarkably different between the two groups. Similarly, the time course of papilloma development was indistinguishable between the HPV8-Tg/*AID*$^{+/+}$ and HPV8-Tg/*AID*$^{-/-}$ mice. Furthermore, AID expression was not induced in the skin papillomatous tissues of the HPV8-Tg/*AID*$^{+/+}$ mice. We conclude that AID is not necessary for the viral protein-induced oncogenesis in these two mouse models.

Methods

Mouse maintenance and genotyping

All the mice used in this study were maintained at the Institute of Laboratory Animals in accordance with the guidelines of the Animal Research Committee, Graduate School of Medicine, Kyoto University. *AID*$^{-/-}$ mice (16) backcrossed to C57/B6 (B6) were crossed with HCV core protein transgenic mouse line (HCV-Tg) (12, 13) and HPV8-Tg mice (on an FVB/N background) (15). AID-Cre and Rosa-RFP compound mice (17) were crossed with HCV-Tg mice to enable the detection of previous and current AID expression. The genotyping primers are described in Supplementary Table 1, available at *International Immunology* Online.

Western blotting

Western blotting was performed by conventional methods. Mouse organs were dissected and homogenized in RIPA buffer. The primary antibodies used were the rat monoclonal anti-mouse AID antibody 2 (MAID-2) (eBioscience, San Diego, CA, USA), anti-Tubulin antibody (Calbiochem, MERCK, Darmstadt, Germany) and anti-HCV core protein antibody (clone B2, Yes Biotech Lab, Anogen, Ontario, Canada).

Reverse transcription–PCR and quantitative reverse transcription–PCR

Mouse organs were excised and homogenized in Sepasol RNA I Super (Nacalai Tesque, Kyoto, Japan) following the manufacturer's instructions. Reverse transcription–PCR (RT–PCR) was performed as previously described (18). ExTaq DNA polymerase (TaKaRa, Shiga, Japan) and the primers described in Supplementary Table 2, available at *International Immunology* Online, were used for conventional PCR. Real-time PCR was performed with the primer sets in Supplementary Table 2, available at *International Immunology* Online, and the Power SYBR Green PCR Master Mix (ABI, Life Technologies Japan, Tokyo, Japan) using the ABI 7900HT system (ABI). The delta-delta Ct method was used to calculate the fold change in gene expression. Error bars show the standard deviation.

Histology and immunohistochemistry

For AID immunohistochemical staining, freshly excised livers were fixed in 4% paraformaldehyde and processed for frozen section as previously described (19). AID protein was detected by MAID-2 and peroxidase-labeled donkey F(ab')2 anti-rat IgG (Jackson ImmunoResearch, West Grove, PA, USA) and stained with diaminobenzidine. Images were

captured with a DM5000B microscope (Leica; Wetzlar, Germany). Hematoxylin and eosin (H&E)-stained samples were fixed with Mildform 10N (Wako Pure Chemical Industries, Osaka, Japan), embedded in paraffin and stained by standard methods.

Liver cell fractionation and FACS analysis

The isolation of intra-hepatic immune cells (IHICs) from the liver of HCV-Tg mice was performed as previously described, with some minor modifications (20). The composition of IHIC cells was assessed by staining with the following antibodies: PE-labeled anti-mouse B220 for B cells, allophycocyanin (APC)-conjugated anti-mouse CD11b for macrophages and FITC-labeled anti-mouse CD8 and APC-anti-mouse CD4 for T cells. The stained cells were analyzed on a FACSCalibur (BD Japan, Tokyo).

ELISA

TNF-α, IL-1β and TGF-β were detected using ELISA kits specific for each cytokine (BioSource, Life Technologies), according to the manufacturer's instructions.

Statistical analysis

The Mann–Whitney *U*-test was used to calculate the statistical differences in AID expression (Fig. 1B). Fisher's exact test was used to determine significant differences in tumor incidence (Table 3). Student's *t*-test was used to determine significant differences in cytokine expression (Fig. 3B and C), and Welch's *t*-test was used for pathological severity validation (Table 2). *P* values < 0.05 were considered statistically significant.

Results

Increased AID transcripts in the liver of HCV-Tg mice

To generate the observation groups, HCV-Tg mice were crossed with *AID*$^{-/-}$ mice. Then HCV-Tg/AID$^{+/-}$(HCV(+)AID$^{+/-}$) mice from the first filial generation were again crossed each other and the obtained HCV(+)AID$^{-/-}$ and HCV(+)AID$^{+/+}$ mice of the second filial generation were compared as the observation groups. The expression level of the HCV core protein in the liver was similar in the HCV(+)AID$^{-/-}$ and HCV(+)AID$^{+/+}$ mice (Supplementary Figure 1, available at *International Immunology* Online). Because HCV-Tg mice develop severe steato-hepatitis within 9 months after birth (12), and this chronic inflammation is supposed to reproduce the similar cytokine environment to the TNF-α-stimulated hepatocyte cell lines that express AID (9), we examined AID expression in the liver. AID transcripts were detected in the liver from 16-month-old HCV(+)AID$^{+/+}$ mice, but not from wild-type B6 mice (Fig. 1A, Supplementary Figure 2, available at *International Immunology* Online). However, the AID expression detected in the HCV(+)AID$^{+/+}$ liver was comparable to the low levels observed in primary unstimulated spleen cells, which included B and T lymphocytes. Transcripts for CD19, a specific marker for B lymphocytes, were also higher in the HCV(+) compared with the B6 liver, suggesting that the HCV(+) liver may contain a considerable number of B

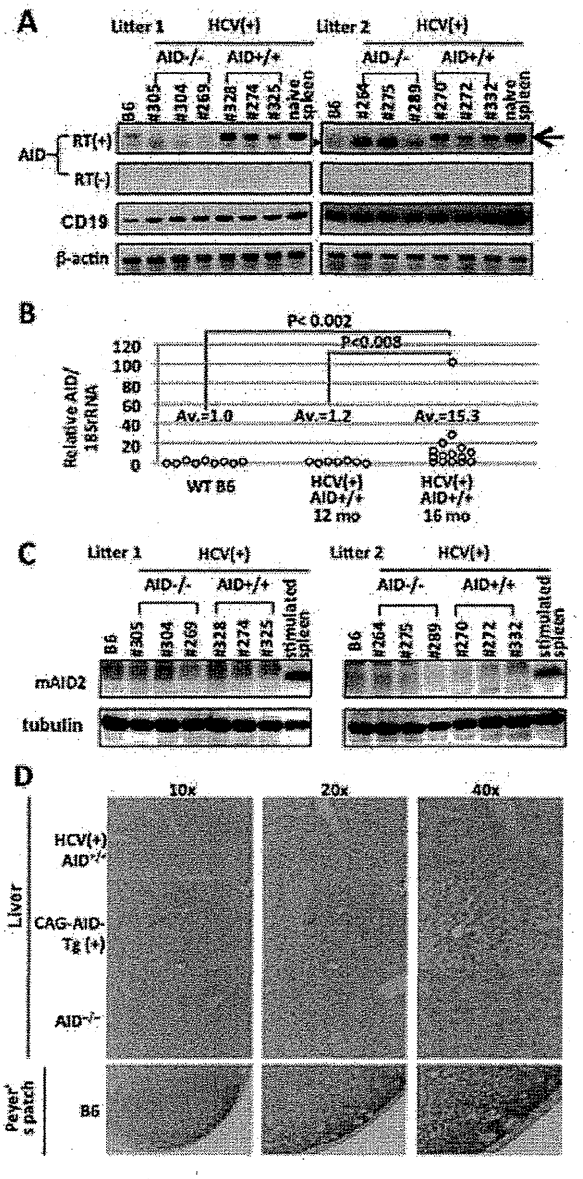

Fig. 1. AID expression in the liver of HCV-Tg mice. (A) Representative RT–PCR analysis showing AID mRNA expression in the liver of 16-month-old HCV(+)AID$^{+/+}$ mice. Naive spleen RNA was included as a positive control. Numbers indicate individual mice. RT(+), with reverse transcriptase; RT(−), without reverse transcriptase. The arrow indicates primer-specific amplification, and the arrowhead shows non-specific amplification. (B) Relative AID expression level in the liver of HCV(+)AID$^{+/+}$ mice at 16 months (n = 15) and 12 months of age (n = 7) and in wild-type (WT) 16-month-old (B6) mice (n = 9), determined by quantitative (q) RT–PCR. *P* value by Mann–Whitney *U*-test. (C) AID protein in the liver of the 16-month-old HCV-Tg mice analyzed in (A), determined by western blot. Splenocytes stimulated with IL-4 and LPS for 3 days were used as a positive control. (D) Immunohistochemistry for AID protein localization in the liver of HCV-Tg mice. The Peyer's patches and liver of a CAG-AID-Tg (CAG promoter-driven AID Tg) mouse were included as positive controls, and the liver of an AID$^{-/-}$ mouse was included as a negative control.

Table 1. AID, CD19 and albumin mRNA levels in purified IHICs and hepatocytes

	CD19/18s rRNA			Albumin/18s rRNA		AID/18s rRNA		
	IHICs	Hepatocytes	Spleen B cells	IHICs	Hepatocytes	IHICs	Hepatocytes	Spleen B cells
B6	326.6	3.3	920.0	1.0	1171.3	7.0±0.30	1.0	338.6±11.7
HCV(+)AID$^{-/-}$	306.1	1.3		0.27	1082.0	0.0	0.0	
HCV(+)AID$^{+/+}$	360.6	1.0		10.6	1027.2	132.6±11.0	3.2±0.63	

Relative AID/18s rRNA expression in B6 hepatocyte is set as 1.0, relative CD19/18s rRNA in HCV(+)AID$^{+/+}$ as 1.0 and relative Albumin/18s rRNA in B6 as 1.0. Zero means undetectable signal by q-PCR.

Table 2. The scored histological phenotypes of HCV(+)AID$^{-/-}$ and HCV(+)AID$^{+/+}$ mice

	Genotype of AID	Severity score				
		0	1	2	3	Average
Steatosis in HCV(+)						
12 months	−/−	0	0	0	3	3
	+/+	0	0	0	2	3
16 months	−/−	2	8	2	0	1.00*
	+/+	0	8	4	0	1.33
20 months	−/−	9	7	1	4	1.00*
	+/+	3	12	2	4	1.33
Lymphoid follicle in HCV(+)						
16 months	−/−	9	3	0	0	0.25*
	+/+	5	7	0	0	0.58
20 months	−/−	4	13	1	3	1.14*
	+/+	2	11	4	4	1.48

The severity of steatosis and lymphoid follicle formation is classified as: 0 (none), 1 (mild), 2 (moderate) or 3 (severe). Values are the numbers of mice with each score.
*AID$^{-/-}$ versus AID$^{+/+}$, $P > 0.05$ by Welch's *t*-test.

Table 3. Liver tumor incidence in HCV-Tg mice

Age	16 months		20 months	
AID genotype	−/−	+/+	−/−	+/+
Male/Female	0/15	0/15	21/0	21/0
Tumour	0	0	3	4
Malignancy	0	0	2	4*

*AID$^{-/-}$ versus AID$^{+/+}$, $P > 0.05$ by Fisher's exact test.

lymphocytes, which could contribute to the increased AID expression. Real-time PCR analysis revealed that the AID transcript level in the liver from 16-month-old HCV(+)AID$^{+/+}$ females was 15-fold greater than that from the liver of similarly aged B6 mice and of 12-month-old HCV(+)AID$^{+/+}$ males (Fig. 1B).

The AID protein levels were measured in the same liver samples by western blotting (Fig. 1C). However, using MAID-2, no protein signal could be detected in the same samples that contained AID transcripts (Fig. 1A). To quantify the limitation of AID protein detection by MAID-2, we used spleen cells as a control (Supplementary Figure 3, available at *International Immunology* Online). We assigned one arbitrary unit of AID mRNA to the q-PCR signal detected from 500 ng of naive spleen cell RNA. Extracts prepared from the same number of spleen cells contained 8.6 μg protein, which did not elicit a detectable AID signal in the western blot. Since the AID transcript level from the HCV(+)AID$^{+/+}$ samples in Supplementary Figure 2, available at *International Immunology* Online, was lower than that in naive spleen cells, we conclude that the AID protein signal in the HCV(+)AID$^{+/+}$ liver was below the level detected by MAID2.

We next explored the possibility that the AID protein expression was limited to a specific location in the liver, such as the immune cells in the hepatic blood vessels. We therefore performed an immunohistochemical analysis of AID (Fig. 1D). Although positive controls including liver tissue from CAG-promoter-driven AID transgenic mice (3) and Peyer's patches from B6 wild-type mice showed clear brownish signals, there was no signal detected in any part of the HCV(+)AID$^{+/+}$ liver tissue samples.

AID transcripts are detected in IHICs, but not in hepatocytes from HCV-Tg mice

We next explored the possibility that the low level of AID transcripts was contributed by B cells infiltrating the HCV-Tg liver. Liver cells from three HCV(+)AID$^{-/-}$ or HCV(+)AID$^{+/+}$ mice at 16 months of age were fractionated to separate the IHICs from the hepatocytes (Fig. 2A and B). RNA was purified from both fractions of each genotype, and the AID, CD19 and albumin transcripts were analyzed to confirm the purity of these fractions and to identify the cellular origin of the AID mRNA (Table 1). CD19 transcripts were detected almost exclusively in IHICs, while albumin transcripts were mostly in hepatocytes, validating the fractionation procedure. The level of AID transcripts detected in the HCV(+)AID$^{+/+}$ IHICs was comparable to the level observed in splenic B cells (132.6±11.0 versus 338.6±11.7, respectively), while the level in hepatocytes was much lower, indicating that the source of AID transcripts in the liver was not the hepatocytes themselves but the IHICs. Cell surface marker analysis by FACS revealed that the IHICs consisted of B220$^+$ B cells (25–29%), CD4$^+$ or CD8$^+$ T cells (~45%) and CD11b$^+$ cells (7–10%), and that this composition was not notably changed by the presence of the HCV transgene or the AID genotype at 16 months of age (Fig. 2A, Supplementary Table 3, available at *International Immunology* Online).

To detect both current and past AID expression, transgenic reporter mice expressing tdRFP under the control of BAC-AID-Cre (17) were crossed to HCV-Tg mice (Fig. 2B and C, Supplementary Table 3, available at *International Immunology* Online). This mouse line reveals tdRFP fluorescence in any cells that have (or had) expressed AID. Using this approach, tdRFP$^+$ cells were found to represent

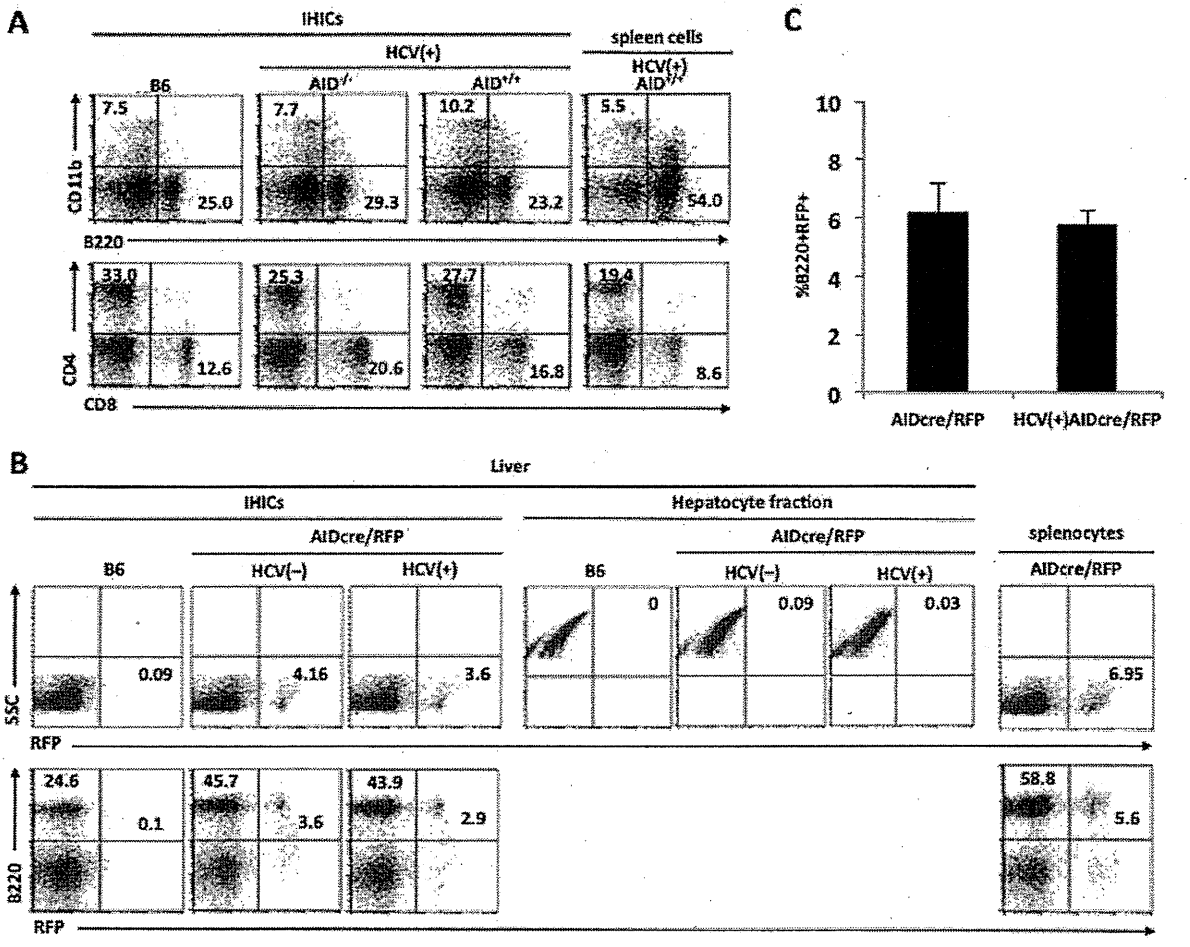

Fig. 2. Cell surface marker analysis of IHICs and hepatocytes from HCV-Tg mice. (A) Cell surface marker profile of IHICs revealed by FACS analysis. The numbers indicate the percentage of each population. The data are representative of three independent experiments. (B) AID expression represented by the tdRFP reporter in the IHICs and hepatocytes from the liver of 3-month-old HCV(+)AIDcre/RFP and HCV(−)AIDcre/RFP mice. The FACS profile data shown in (B and C) are representative of three independent experiments. The definitive cell numbers of each quadrant in (B and C) are shown in Supplementary Table 3, available at *International Immunology* Online. (C) Average percentage of $B220^{+}RFP^{+}$ cells in the $B220^{+}$ IHIC population from three independent experiments.

3–4% of the total IHICs in both HCV-Tg and no HCV-Tg (HCV(−)) mice at 3 months of age (Fig. 2B). tdRFP was not detected in hepatocytes from 3-month-old HCV(+) mice that had already developed mild steato-hepatitis (12). Analysis of three mice of each genotype (HCV(+) and HCV(−)) revealed that the $tdRFP^{+}$ cells represented $5.8 \pm 0.45\%$ versus $6.2 \pm 1.0\%$ of the $B220^{+}$ population, respectively (Fig. 2C), indicating that the presence of the HCV transgene did not affect the AID gene expression in mice during the first 3 months of life.

AID deficiency reduces the severity of histopathological phenotypes and cytokine expression profiles in the liver of HCV-Tg mice

It is reported that 14–30% of HCV-Tg male mice develop HCC between 16 and 19 months of age (13). We therefore analyzed the histopathological phenotypes of H&E-stained liver sections from $HCV(+)AID^{-/-}$ and $HCV(+)AID^{+/+}$ mice at 12 (male), 16 (female) and 20 months (male) of age (Figs 3A and 4A and Table 2). The severities of steatosis and lymphocyte infiltration were graded from 0 to 3, and the average scores for each group were calculated and tested by Welch's *t*-test (Table 2).

At 12 months of age, both $HCV(+)AID^{-/-}$ and $HCV(+)AID^{+/+}$ male mice had developed severe steatosis. Unexpectedly, the steatosis was milder in both $HCV(+)AID^{-/-}$ and $HCV(+)AID^{+/+}$ female mice at 16 months of age than $HCV(+)AID^{-/-}$ and $HCV(+)AID^{+/+}$ male mice at 12 months of age. The steatosis in the $HCV(+)AID^{+/+}$ mice appeared to be more severe than in $HCV(+)AID^{-/-}$ mice, but the difference was not significant ($P > 0.05$). This decrease in steatosis severity may have been due to the female composition of the mice because females of this HCV-Tg line did not show tumor development

(13), and human HCV-infected cirrhotic females develop HCC less frequently (21). In addition, lymphoid follicle formation was apparent at 16 months of age and was more frequent in the HCV(+)AID$^{+/+}$ than the HCV(+)AID$^{-/-}$ mice (Fig. 3A; Table 2). Consistent with the previous report (13), the fibrotic or regenerative nodular changes were very mild at 16 months of age.

However, the liver samples from both HCV(+)AID$^{-/-}$ and HCV(+)AID$^{+/+}$ mice at 20 months of age revealed marked progressive changes, with nuclear atypia detected in 10 out of 21 of each genotype, and liver cell degeneration or regenerative changes detected in 10 and 11 out of 21 HCV(+)AID$^{-/-}$ and HCV(+)AID$^{+/+}$ mice, respectively (Fig. 4A). Interestingly, both the steatosis and lymphoid follicle severity scores appeared to be higher in the HCV(+)AID$^{+/+}$ than the HCV(+)AID$^{-/-}$ 20-month-old mice (1.33 versus 1.00 for steatosis and 1.48 versus 1.14 for lymphoid follicles, respectively) although the observed differences were not statistically significant (Table 2).

We next examined whether the more advanced inflammatory histological phenotypes observed in the HCV(+)AID$^{+/+}$ mice were associated with increases in cytokine expression. Since cytokine production levels are altered in chronic HCV hepatitis (22) and in HCV-Tg mouse (23), we used q-PCR to measure representative pro-inflammatory T_h1 and T_h2 cytokine expression levels in the livers of 16-month-old female mice (Fig. 3B). The presence of the HCV transgene was associated with significantly higher levels of IL-1β, TNF-α and TGF-β mRNA, and HCV(+)AID$^{+/+}$ mice exhibited higher TNF-α levels than HCV(+)AID$^{-/-}$ mice. Consistent with the q-PCR results, the protein levels of IL-1β and TGF-β were also elevated by the presence of the HCV transgene, and the TNF-α protein production level was dependent on the presence of AID, suggesting that TNF-α production may have led to the aggressive pathological findings observed in HCV(+)AID$^{+/+}$ mice (Fig. 3C).

Similar tumor incidence in HCV(+)AID$^{-/-}$ and HCV(+) AID$^{+/+}$ mice

The incidence of tumor formation was carefully examined by histopathological and macroscopic evaluation. None of the 15 HCV(+)AID$^{-/-}$ or 15 HCV(+)AID$^{+/+}$ 16-month-old female mice showed evidence of liver tumor formation, consistent with a previous report (Table 3) (13). Further analysis of the 20-month-old male groups, including 21 HCV(+)AID$^{-/-}$ and 21 HCV(+) AID$^{+/+}$ mice, revealed that 4 out of 21 HCV(+)AID$^{+/+}$ mice carried macroscopic tumors, all of which were determined to be malignant by histological examination (Fig. 4A, right 4 panels). Similarly, 3 out of 21 HCV(+)AID$^{-/-}$ mice bore macroscopic tumors, two of which were judged to be malignant (Fig. 4A, left 3 panels). These results suggest that AID is not essential for HCV-induced carcinogenesis. Consistent with these findings, the AID transcript level in the tumor region of an AID$^{+/+}$ mouse (#241) was equivalent to the level detected in a non-tumor area (Fig. 4B). Comparison of the AID expression in the tumor and non-tumor areas from the two tumor-bearing mice of the HCV(+)AID$^{-/-}$ and the two of HCV(+)AID$^{+/+}$ indicated that the tumor tissues did not contain elevated AID expression levels (Fig. 4C). The AID protein levels were not detectable by western blotting in either the tumor or non-tumor areas (Fig. 4D).

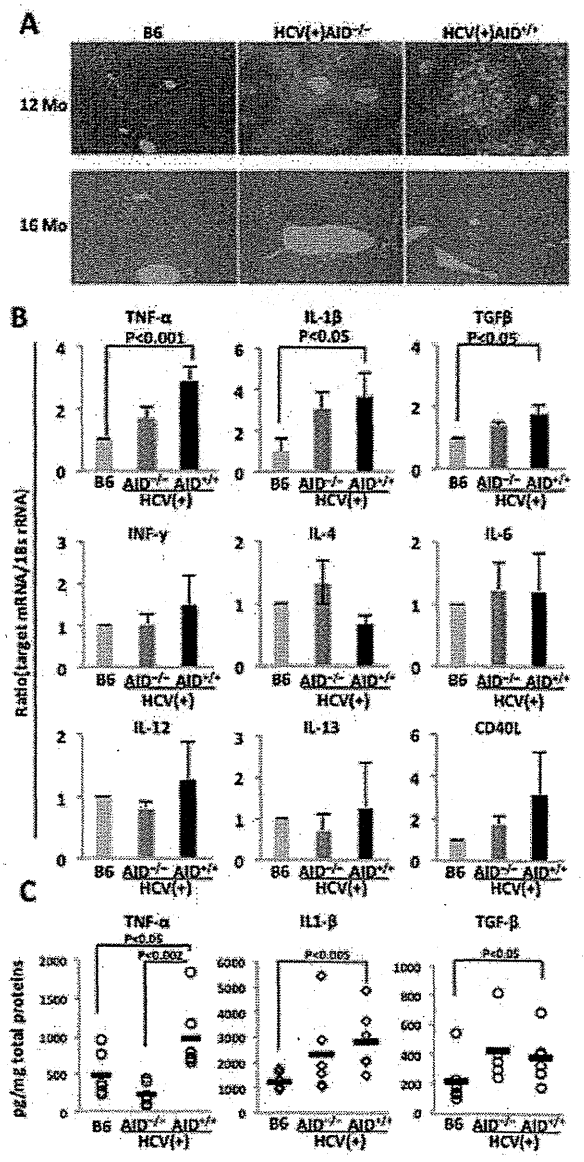

Fig. 3. Inflammatory responses in the liver of HCV(+)AID$^{-/-}$ and HCV(+)AID$^{+/+}$ mice. (A) Representative liver histology shown by H&E staining. Wild-type B6 mice (left panel), HCV(+)AID$^{-/-}$ (middle panel) and HCV(+)AID$^{+/+}$ (right panel) mice at 12 and 16 months of age (original magnification ×200). (B) mRNA expression of pro-inflammatory, T_h1 and T_h2 cytokines in the liver of 16-month-old mice. $n = 3$ (mean ± SD). (C) ELISA detection of cytokines in whole liver lysates from 16-month-old wild-type B6, HCV(+)AID$^{-/-}$ and HCV(+)AID$^{+/+}$ mice. The data shown for each of the groups are based on the values from six mice, except for the IL1-β evaluation for the HCV(+)AID$^{+/+}$ group, which is based on five mice.

Dispensability of AID for the development of skin tumors in HPV8-Tg mice

To examine AID's involvement in the development of HPV8-induced skin tumors, HPV8-Tg (HPV(+)) mice were crossed with AID$^{-/-}$ mice. Then HPV8(+)AID$^{+/-}$ mice of the first filial

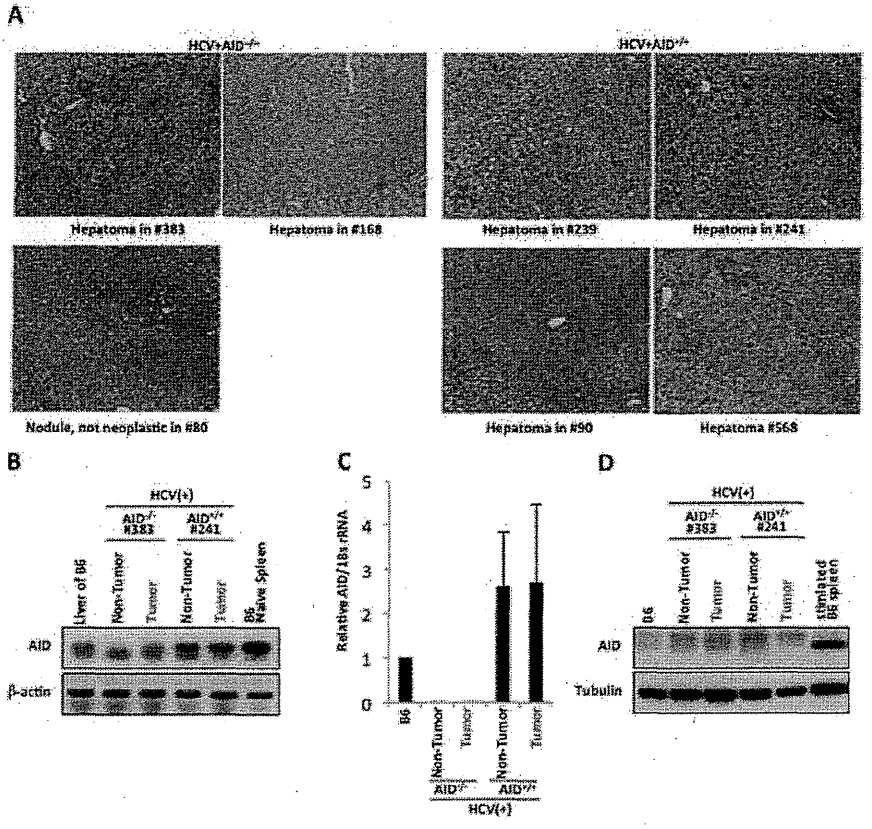

Fig. 4. Development of hepatocellular carcinoma in HCV-Tg mice. (A) H&E staining of the tumors found in HCV(+)AID$^{+/+}$ and HCV(+)AID$^{-/-}$ mice (original magnification ×200). (B) Representative AID mRNA expression profile in the tumor and non-tumor regions of HCV(+)AID$^{-/-}$ (#383) and HCV(+)AID$^{+/+}$ (#241) mice. (C) Quantitative RT–PCR of AID mRNAs analyzed as in (B). Error bars show standard deviation from two mice of each group. (D) Western blot analysis of AID protein in samples from the same mice analyzed in (B).

generation were again crossed each other and the obtained HPV8(+)AID$^{-/-}$ and HPV8(+)AID$^{+/+}$ mice of the second filial generation were compared as the observation groups. Both genotypes developed skin tumors, and tumor samples from 6-month-old mice were tested for AID expression by RNA and protein analyses (Fig. 5A and B). Neither the AID protein nor its RNA was detectable in the samples analyzed. After 6 months, the final skin tumor prevalence was ~30% in both mouse populations (15 out of 49 HPV8(+)AID$^{-/-}$ and 16 out of 51 HPV8(+)AID$^{+/+}$) (Supplementary Table 4, available at *International Immunology* Online), and the frequency and time course of tumor development in the two groups were almost indistinguishable (Fig. 5C). The histological examination of the skin tumor did not show any difference between HPV8(+)AID$^{+/+}$ and HPV8(+)AID$^{-/-}$ mice (Fig. 5D). The lower papilloma prevalence (~30%) compared to the original report describing the HPV8(+) mice (15) may be due to the mixed genetic background of FVB/N and B6 in both groups (the HPV8(+)AID$^{-/-}$ and HPV8(+)AID$^{+/+}$ mice), since mice with an FVB/N genetic background are reported to have more severe papilloma progression than those with a B6 background (15). Although the malignant progression to SCC in these skin tumors was not examined, AID expression was absent, and tumor development was equivalent in the AID$^{-/-}$ and AID$^{+/+}$ mice. We thus conclude that AID is not involved in HPV8-induced skin tumorigenesis.

Discussion

In this study, we investigated the requirement of AID for virally induced tumorigenesis by using compound mice that were generated by crossing mice transgenic for either HCV core proteins or HPV8 early proteins with either AID wild-type or knockout mice. Our results indicated that AID was expressed in neither hepatocytes of HCV-Tg nor skin tissue of HPV8-Tg. Thus, AID was not shown to be required for the development of both HCV- and HPV8-promoted tumorigenesis. We could not conclude that the frequency of the liver malignancy is statistically different between HCV(+)AID$^{+/+}$ (4 out of 21 mice) and HCV(+)AID$^{-/-}$ (2 out of 21 mice), partly because the frequency of the liver malignancy was unexpectedly lower than that in the original report (13). Studies on 5 times the number of mice may allow us to obtain statistically significant conclusions about the frequency of the liver malignancy between HCV(+)AID$^{+/+}$ and HCV(+)AID$^{-/-}$ mice. We note, however, that the HCV(+)AID$^{+/+}$ mice exhibited higher levels of TNF-α

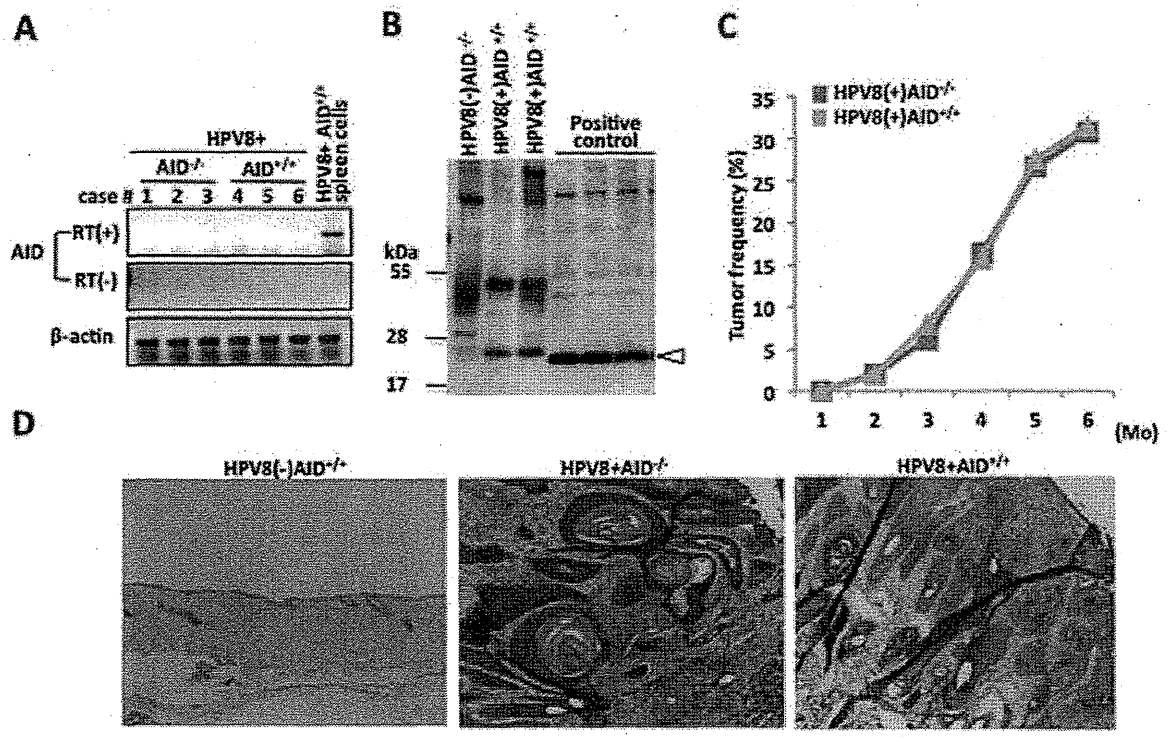

Fig. 5. Cutaneous papilloma in HPV8(+)AID$^{-/-}$ and HPV8(+)AID$^{+/+}$ mice. (A) Representative results of the RT–PCR analysis of AID mRNA in skin tumors of HPV8(+)AID$^{-/-}$ (cases 1, 2, 3) and HPV8(+)AID$^{+/+}$ (cases 4, 5, 6) littermates, and a positive control (naive spleens of HPV8(+)AID$^{+/+}$ mice). The data shown are representative of three independent experiments (n = 9 for each group). (B) Representative results of western blots detecting AID protein in lysates of skin tumors from HPV8(+)AID$^{+/+}$ mice. The negative control was skin tissue from HPV8-Tg negative AID$^{-/-}$, and the positive control was a lysate of spleen cells from HPV8(+)AID$^{+/+}$ mice that was cultured with LPS and IL-4 for 3 days. The arrowhead shows the specific band of AID protein. (C) Papilloma frequency after birth in HPV8(+)AID$^{-/-}$ and HPV8(+)AID$^{+/+}$ mice. (D) H&E staining of skin tissues from HPV8(+)AID$^{+/+}$ and HPV8(+)AID$^{-/-}$ mice.

production with more severe histological phenotypes than the HCV(+)AID$^{-/-}$ mice.

AID is reported to be expressed in HCC and in the surrounding non-cancerous liver tissues (6, 7). In addition, the hepatoma-derived cell lines HepG2, Hep3B and Huh-7 have all been shown to express AID in response to HCV core protein-induced NF-κB signaling (9). It therefore has been assumed that AID is induced in HCV-Tg mice and contributes to liver carcinogenesis. However, AID expression was not detected in HCV core protein-positive hepatocytes, and the low levels of AID transcripts in liver tissues were attributable to infiltrating B cells in this study. The different AID expression levels observed in the present mouse model and HCV-infected patients could be due in part to pathogenic differences between the two systems. HCV-Tg mice lack cirrhotic changes (12, 13), which may be involved in inducing AID expression. In contrast, the natural course of human HCV infection leads to chronic hepatitis development, with bile duct damage and steatosis in the majority of patients (24), and the failure of virus eradication leads to liver cirrhosis and/or HCC (25). In human cases, 80–90% of the HCC develops from cirrhotic liver tissues (21), indicating that chronic inflammatory reactions generally contribute to carcinogenesis.

The involvement of B and T cells in liver injury via autoimmune antibody may be a possible reason for the strong inflammatory response in some part of natural HCV infection cases (26–28). CD81, an HCV-binding molecule, is expressed on the surface of B and T cells and both type of lymphocyte may be infected by HCV (28, 29). HCV infection of B cells causes the development of non-organ-specific auto-antibodies (NOSAs) and cryoglobulinemia (26, 30). In the various NOSAs, some antibodies add auto-antibody-mediated liver injury to viral hepatitis (30). For example, anti-liver/kidney microsomal antibody type 1 (LKM1) and anti-smooth muscle antibody (SMA) are also found in autoimmune hepatitis, and anti-microsomal antibody (AMA) is closely related to primary biliary cirrhosis (31). These liver-targeting antibodies of NOSAs are proposed to be produced based on the mimicry of autoantigens by HCV polyproteins including NS3, 4 and 5 in addition to core proteins (32). In the current HCV-Tg mouse model, auto-antibody-dependent liver injury is less likely because only the core of the HCV polyprotein is expressed and HCV infection in B cells is absent. The absence of this extra-hepatic complication partly explains the reasons why the inflammation is weak in this study compared to natural HCV infection and why AID is not expressed in the hepatocytes of HCV-Tg mouse.

The discrepancy of AID expression between the current animal study and the natural HCV infection could be also due to different regulation of AID expression between mouse and human hepatocytes. The transcriptional regulation of AID expression in B lymphocytes has been extensively examined both *in vitro* and *in vivo* and shown to depend on B-cell-specific and environmental stimulus-specific factors (33). The latter include Stat6 and NF-κb, which are activated by viral infection. AID was activated by transfected HCV core protein responding to the NF-κB signaling pathway (9) in human cell lines; however, NF-κB is not activated in the current HCV-Tg model whereas the upstream TNF-α signal is increased (23). Although the difference in the AID promoter between human and mice is not known, we cannot totally exclude this possibility to explain the different AID expression response.

Although HCV-Tg had weaker inflammatory responses than natural HCV infection, the inflammation observed in HCV(+) $AID^{+/+}$ mice tended to be more severe than that in HCV(+) $AID^{-/-}$ mice. The HCV core protein expression induced infiltration of IHICs including T, B and probably NK cells, and $AID^{+/+}$ B cells enhanced TNF-α production more than $AID^{-/-}$ B cells. The mechanism of TNF-α up-regulation by AID is unknown; however, higher levels of TNF-α production are likely to affect the pathogenesis or prognosis. TNF-α and IL-1β were increased in the whole liver lysates of 16-month-old HCV-Tg mice, as previously reported (23). Clinically, increased TNF-α production from liver-infiltrating monocytes in Non-A, Non-B hepatitis has also been reported (34). Furthermore, TNF-α was shown to activate the AP-1 pathway (23), which promotes cell proliferation (35).

The HCC development without severe 'cirrhotic' findings may be due to carcinogenic properties associated with the HCV core protein, including suppression of apoptosis (by interacting with p53 and pRb), promotion of proliferation (by up-regulating the Wnt/b-catenin and Raf/MAPK pathways) and induction of reactive oxygen species (10, 36).

Stat3 is essential for HPV8-induced skin carcinogenesis (37). The Stat6 and Stat3 DNA recognition motifs are not completely identical, but share partial homology (38). We suspected that HPV8 induces AID through Stat and NF-κB signaling pathways and examined AID's involvement in the HPV8-Tg mouse model. Contrary to our expectation, AID expression was not induced in the HPV8-Tg mouse model, which developed papilloma at a frequency of 30%. Since we observed these mice only up to 6 months before SCC development, we cannot rule out the possibility that AID in the skin squamous cells is induced later to convert papilloma to SCC.

In conclusion, our results suggest that AID may not be essential for either HCV-induced liver carcinogenesis or HPV8-induced papillomagenesis. We were unable to detect AID expression in transgenic cells expressing viral oncogenic proteins in either model, contrary to expectations. These results indicate that the expression of AID is strictly regulated in both hepatocytes and cutaneous keratinocytes at least in the mouse models used here.

Supplementary data

Supplementary data are available at *International Immunology* Online.

Funding

Ministry of Education, Culture, Sports, Science and Technology of Japan Grant-in-Aid for Specially Promoted Research (17002015 to T.H.); Grant-in-Aid for Scientific Research (C) (25440007 to M.K.).

Acknowledgements

We thank Prof. Tsutomu Chiba for helpful discussions, Prof. Hitoshi Nagaoka for useful suggestions, Dr Le Thi Huong for technical assistance and Mrs Mikiyo Nakata for providing HepG2 cells.

References

1 Honjo, T., Kinoshita, K. and Muramatsu, M. 2002. Molecular mechanism of class switch recombination: linkage with somatic hypermutation. *Annu. Rev. Immunol.* 20:165.

2 Nagaoka, H., Tran, T. H., Kobayashi, M., Aida, M. and Honjo, T. 2010. Preventing AID, a physiological mutator, from deleterious activation: regulation of the genomic instability that is associated with antibody diversity. *Int. Immunol.* 22:227.

3 Okazaki, I. M., Hiai, H., Kakazu, N. *et al.* 2003. Constitutive expression of AID leads to tumorigenesis. *J. Exp. Med.* 197:1173.

4 Matsumoto, Y., Marusawa, H., Kinoshita, K. *et al.* 2007. Helicobacter pylori infection triggers aberrant expression of activation-induced cytidine deaminase in gastric epithelium. *Nat. Med.* 13:470.

5 Machida, K., Cheng, K. T., Sung, V. M. *et al.* 2004. Hepatitis C virus induces a mutator phenotype: enhanced mutations of immunoglobulin and protooncogenes. *Proc. Natl Acad. Sci. USA* 101:4262.

6 Kou, T., Marusawa, H., Kinoshita, K. *et al.* 2007. Expression of activation-induced cytidine deaminase in human hepatocytes during hepatocarcinogenesis. *Int. J. Cancer* 120:469.

7 Vartanian, J. P., Henry, M., Marchio, A. *et al.* 2010. Massive APOBEC3 editing of hepatitis B viral DNA in cirrhosis. *PLoS Pathog.* 6:e1000928.

8 Ishikawa, C., Nakachi, S., Senba, M., Sugai, M. and Mori, N. 2011. Activation of AID by human T-cell leukemia virus Tax oncoprotein and the possible role of its constitutive expression in ATL genesis. *Carcinogenesis* 32:110.

9 Endo, Y., Marusawa, H., Kinoshita, K. *et al.* 2007. Expression of activation-induced cytidine deaminase in human hepatocytes via NF-kappaB signaling. *Oncogene* 26:5587.

10 Tsai, W. L. and Chung, R. T. 2010. Viral hepatocarcinogenesis. *Oncogene* 29:2309.

11 McGivern, D. R. and Lemon, S. M. 2011. Virus-specific mechanisms of carcinogenesis in hepatitis C virus associated liver cancer. *Oncogene* 30:1969.

12 Moriya, K., Yotsuyanagi, H., Shintani, Y. *et al.* 1997. Hepatitis C virus core protein induces hepatic steatosis in transgenic mice. *J. Gen. Virol.* 78 (Pt 7):1527.

13 Moriya, K., Fujie, H., Shintani, Y. *et al.* 1998. The core protein of hepatitis C virus induces hepatocellular carcinoma in transgenic mice. *Nat. Med.* 4:1065.

14 Akgül, B., Cooke, J. C. and Storey, A. 2006. HPV-associated skin disease. *J. Pathol.* 208:165.

15 Schaper, I. D., Marcuzzi, G. P., Weissenborn, S. J. *et al.* 2005. Development of skin tumors in mice transgenic for early genes of human papillomavirus type 8. *Cancer Res.* 65:1394.

16 Muramatsu, M., Kinoshita, K., Fagarasan, S., Yamada, S., Shinkai, Y. and Honjo, T. 2000. Class switch recombination and hypermutation require activation-induced cytidine deaminase (AID), a potential RNA editing enzyme. *Cell* 102:553.

17 Qin, H., Suzuki, K., Nakata, M. *et al.* 2011. Activation-induced cytidine deaminase expression in CD4+ T cells is associated with a unique IL-10-producing subset that increases with age. *PLoS ONE* 6:e29141.

18 Kobayashi, M., Aida, M., Nagaoka, H. *et al.* 2009. AID-induced decrease in topoisomerase 1 induces DNA structural alteration

and DNA cleavage for class switch recombination. *Proc. Natl Acad. Sci. USA* 106:22375.
19 Takai, A., Toyoshima, T., Uemura, M. *et al.* 2009. A novel mouse model of hepatocarcinogenesis triggered by AID causing deleterious p53 mutations. *Oncogene* 28:469.
20 Blom, K. G., Qazi, M. R., Matos, J. B., Nelson, B. D., DePierre, J. W. and Abedi-Valugerdi, M. 2009. Isolation of murine intrahepatic immune cells employing a modified procedure for mechanical disruption and functional characterization of the B, T and natural killer T cells obtained. *Clin. Exp. Immunol.* 155:320.
21 Fattovich, G., Stroffolini, T., Zagni, I. and Donato, F. 2004. Hepatocellular carcinoma in cirrhosis: incidence and risk factors. *Gastroenterology* 127(5 Suppl 1):S35.
22 Castello, G., Scala, S., Palmieri, G., Curley, S. A. and Izzo, F. 2010. HCV-related hepatocellular carcinoma: from chronic inflammation to cancer. *Clin. Immunol.* 134:237.
23 Tsutsumi, T., Suzuki, T., Moriya, K. *et al.* 2002. Alteration of intrahepatic cytokine expression and AP-1 activation in transgenic mice expressing hepatitis C virus core protein. *Virology* 304:415.
24 Bach, N., Thung, S. N. and Schaffner, F. 1992. The histological features of chronic hepatitis C and autoimmune chronic hepatitis: a comparative analysis. *Hepatology* 15:572.
25 World Health Organization (WHO). 2013. *Hepatitic C fact Sheet* No 164. Media Centre.
26 Sansonno, D., Tucci, F. A., Lauletta, G. *et al.* 2007. Hepatitis C virus productive infection in mononuclear cells from patients with cryoglobulinaemia. *Clin. Exp. Immunol.* 147:241.
27 Himoto, T. and Nishioka, M. 2008. Autoantibodies in hepatits C virus-related chronic liver disease. *Hepatitis Monthly* 8:295.
28 Deng, J., Dekruyff, R. H., Freeman, G. J., Umetsu, D. T. and Levy, S. 2002. Critical role of CD81 in cognate T-B cell interactions leading to Th2 responses. *Int. Immunol.* 14:513.
29 Zhang, J., Randall, G., Higginbottom, A., Monk, P., Rice, C. M. and McKeating, J. A. 2004. CD81 is required for hepatitis C virus glycoprotein-mediated viral infection. *J. Virol.* 78:1448.
30 Bogdanos, D. P., Mieli-Vergani, G. and Vergani, D. 2005. Non-organ-specific autoantibodies in hepatitis C virus infection: do they matter? *Clin. Infect. Dis.* 40:508.
31 Zeman, M. V. and Hirschfield, G. M. 2010. Autoantibodies and liver disease: uses and abuses. *Can. J. Gastroenterol.* 24:225.
32 Gregorio, G. V., Choudhuri, K., Ma, Y. *et al.* 2003. Mimicry between the hepatitis C virus polyprotein and antigenic targets of nuclear and smooth muscle antibodies in chronic hepatitis C virus infection. *Clin. Exp. Immunol.* 133:404.
33 Tran, T. H., Nakata, M., Suzuki, K. *et al.* 2010. B cell-specific and stimulation-responsive enhancers derepress Aicda by overcoming the effects of silencers. *Nat. Immunol.* 11:148.
34 Yoshioka, K., Kakumu, S., Arao, M. *et al.* 1990. Immunohistochemical studies of intrahepatic tumour necrosis factor alpha in chronic liver disease. *J. Clin. Pathol.* 43:298.
35 Shaulian, E. and Karin, M. 2001. AP-1 in cell proliferation and survival. *Oncogene* 20:2390.
36 Liang, T. J. and Heller, T. 2004. Pathogenesis of hepatitis C-associated hepatocellular carcinoma. *Gastroenterology* 127(5 Suppl 1):S62.
37 De Andrea, M., Rittà, M., Landini, M. M. *et al.* 2010. Keratinocyte-specific stat3 heterozygosity impairs development of skin tumors in human papillomavirus 8 transgenic mice. *Cancer Res.* 70:7938.
38 Ehret, G. B., Reichenbach, P., Schindler, U. *et al.* 2001. DNA binding specificity of different STAT proteins. Comparison of in vitro specificity with natural target sites. *J. Biol. Chem.* 276:6675.

Hepatology Research

Hepatology Research 2014 doi: 10.1111/hepr.12275

Original Article

Effect of the infectious dose and the presence of hepatitis C virus core gene on mouse intrahepatic CD8 T cells

Yutaka Horiuchi,[1] Akira Takagi,[1] Nobuharu Kobayashi,[1] Osamu Moriya,[1] Toshinori Nagai,[2] Kyoji Moriya,[3] Takeya Tsutsumi,[3] Kazuhiro Koike[3] and Toshitaka Akatsuka[1]

Departments of [1]Microbiology and [2]Pathology, Saitama Medical University, Saitama, and [3]Department of Gastroenterology, Graduate School of Medicine, The University of Tokyo, Tokyo, Japan

Aim: Chronic hepatitis C viral (HCV) infections often result in ineffective CD8 T-cell responses due to functional exhaustion of HCV-specific T cells. However, how persisting HCV impacts CD8 T-cell effector functions remains largely unknown. The aim of this study is to examine the effect of the infectious dose and the presence of HCV core gene.

Methods: We compared responses of intrahepatic CD8 T cells during infection of wild-type or HCV core transgenic (Tg) mice with various infectious doses of HCV-NS3-expressing recombinant adenovirus (Ad-HCV-NS3).

Results: Using major histocompatibility complex class I tetramer and intracellular interferon (IFN)-γ staining method to track HCV-NS3-specific CD8 T cells, we found that a significant expansion of HCV-NS3-specific CD8 T cells was restricted to a very narrow dosage range. IFN-γ production by intrahepatic CD8 T cells in HCV core Tg mice was suppressed as compared with wild-type mice. Higher levels of expression of regulatory molecules, Tim-3 and PD-1, by intrahepatic CD8 T cells and PD-L1 by intrahepatic antigen-presenting cells were observed in HCV core Tg mice following Ad-HCV-NS3 infection, and the expression increased dependent on infectious dose. Furthermore, we found a significant inverse correlation between the percentages of IFN-γ-producing cells and expression of regulatory molecules in antigen-specific intrahepatic CD8 T cells.

Conclusion: High infectious dose and the presence of HCV core gene were strongly involved in ineffective CD8 T-cell responses. We consider that HCV core Tg mouse infected with high infectious dose of Ad-HCV-NS3 is useful as a chronic infection model in the development of immunotherapy for chronic hepatitis C.

Key words: core, functional exhaustion, hepatitis C, infectious dose, T cell

INTRODUCTION

HEPATITIS C VIRUS (HCV) is a positive-sense single-stranded RNA virus of the genus *Hepacivirus* in the family *Flaviviridae*, and it infects 170 million people worldwide.[1] Approximately 10–60% of the patients clear HCV spontaneously during the acute phase of infection,[2] while the others develop chronic persistent HCV infection that eventually leads to liver cirrhosis and hepatocellular carcinoma.[3] HCV-specific cytotoxic T lymphocytes (CTL) play a major role in viral control during acute infection.[4] Nevertheless, during persistent infection, HCV-specific CTL effector functions are significantly impaired.

T-cell exhaustion is one of the remarkable features of chronic HCV infection. In chronically HCV-infected individuals, the frequencies of CTL are relatively low; similarly, the proliferative capacity as well as effector functions of HCV-specific T cells are impaired, and the production of type I cytokines (i.e. interleukin-2 and interferon [IFN]-γ) is dramatically suppressed.[5–8]

It appears that the major factors which determine duration and magnitude of an antiviral immune response are antigen (Ag) localization, dose and kinetics.[9] For example, high doses of widely disseminating strains of lymphocytic choriomeningitis virus (LCMV) exhaust antiviral CTL leading to establishment of a persistent infection.[10] Physical deletion of anti-LCMV CTL is most likely preceded by their functional impairment with the inability to produce effector cytokines.[11,12]

Correspondence: Professor Toshitaka Akatsuka, Department of Microbiology, Faculty of Medicine, Saitama Medical University, 38 Morohongo, Moroyama-cho, Iruma-gun, Saitama 350-0495, Japan. Email: akatsuka@saitama-med.ac.jp

Received 21 May 2013; revision 8 November 2013; accepted 11 November 2013.

Moreover, Wherry *et al.* showed that not only the persistence of a viral Ag, but also the initial Ag level is an important factor determining the quality of the antiviral memory response.[13]

Hepatitis C virus core protein has been reported to suppress T-cell response. HCV core-mediated inhibition of T-cell response can occur via either modulation of pro-inflammatory cytokine production by antigen-presenting cells (APC; i.e. monocyte and dendritic cells)[14] or direct effect on T cells.[15–17] Because the liver is the major site of HCV infection, it is crucial to understand the regulation of host immunity by HCV core in the liver compartment and the impact of HCV core-induced immune dysregulation in facilitating HCV persistence.

Hepatitis C virus does not infect small laboratory animals. The lack of a small animal model has hampered studies attempting to elucidate the mechanism of HCV-mediated suppression of antiviral CD8 T-cell activity and caused difficulty in the development of a therapeutic and/or prophylactic HCV vaccine.

Adenoviral vectors efficiently and reproducibly transfer foreign DNA into the livers of immunocompetent experimental animals. i.v. administration of adenoviral vectors of more than 10^9 infectious units/mouse results in infection and Ag expression in more than 90% of hepatocytes and acute self-limiting viral hepatitis.[18,19]

In this study, to develop a useful animal model in the development of immunotherapy for chronic hepatitis C, we examined the responses of intrahepatic CD8 T cells of HCV core transgenic (Tg) mice with various infectious doses of HCV-NS3-recombinant adenovirus (Ad-HCV-NS3).

METHODS

Mice

C57BL/6 MICE WERE purchased from Clea Japan (Tokyo, Japan), and Tokyo Laboratory Animal Science (Tokyo, Japan). Production of HCV core Tg mice has been described.[20] The core gene of HCV placed downstream of a transcriptional regulatory region from hepatitis B virus, which has been shown to allow an expression of genes in Tg mice without interfering with mouse development,[21] was introduced into C57BL/6 mouse embryos (Clea Japan). Eight- to 10-week-old mice were used for all experiments. The mice were housed in appropriate animal care facilities at Saitama Medical University (Saitama, Japan) and were handled according to international guidelines. The experimental protocols were approved by the Animal Research Committee of Saitama Medical University (#855).

HCV-NS3 recombinant adenovirus

Adenovirus HCV-NS3 expressing the fusion protein, comprising the entire HCV-NS3 and 3X flag, was constructed by using the AdEasy XL adenoviral vector system (Agilent Technologies, Santa Clara, CA, USA). The HCV-NS3 gene corresponding to amino acid residues 1027–1657 was amplified from the plasmid pBRTM/HCV1-3011con which contains the entire DNA sequence derived from the HCV H77 clone (kindly provided by Charls M. Rice, The Rockefeller University, New York, NY, USA)[22] by polymerase chain reaction. The recombinant Ad-HCV-NS3 vector was linearized by PacI digestion, and then transfected into 293 cells using Lipofectamine LTX (Invitrogen, Carlsbad, CA, USA) to generate adenovirus. Ad-HCV-NS3 expressing transgene NS3 was amplified in 293 cells, purified by a series of cesium chloride ultracentrifugation gradients and stored at −80 °C until use. Mice were injected i.v. with 2×10^7, 1×10^9 and 1×10^{10} plaque-forming units (PFU) of Ad-HCV-NS3 or Adψ5 control vector. The experimental protocol regarding construction of recombinant adenovirus and infection of mice was approved by the Recombinant DNA Advisory Committee of Saitama Medical University (#1073).

Isolation of intrahepatic leukocytes

The liver was perfused with phosphate-buffered saline (PBS) plus 0.05% collagenase via the portal vein. Perfused livers were smashed through a 100-μm cell strainer (BD Biosciences, San Jose, CA, USA). The cell suspension was centrifuged with 35% Percoll at 320 *g* for 10 min, and the cell pellet was cultured in a plastic Petri dish in RPMI-1640 medium supplemented with 10% fetal calf serum (FCS; R-10) for 1.5 h to remove adherent cells. Then, non-adherent cells were harvested, washed twice with R-10 and used as intrahepatic lymphocytes (IHL). Adherent cells were used as intrahepatic APC).

Intracellular IFN-γ staining

The IHL were resuspended in R-10. In each well of a 96-well round-bottomed plate, 2×10^6 IHL were incubated for 5 h at 37 °C in R-10 containing 50 ng/mL phorbol myristate acetate (PMA; Sigma-Aldrich, St Louis, MI, USA), 1 μM ionophore A23187 (Sigma-Aldrich) and 1 μg/mL brefeldin-A (BD Biosciences). The cells were then washed twice with ice-cold PBS (−) and incubated for 10 min at 4 °C with a rat antimouse

CD16/CD32 monoclonal Ab (mAb; Fc Block; BD Biosciences) at a concentration of 1 μg/well. Following incubation, the cells were washed twice with ice-cold PBS (–) and stained with a PE-conjugated HCV-NS3 H-2Db tetramer (Tet-603; GAVQNEVTL; Medical and Biological Laboratories, Nagoya, Japan)[23] and peridinin chlorophyll protein (PerCP)-conjugated rat antimouse CD8 MAb (clone 53-6.7; BD Biosciences) for 30 min at 4°C in staining buffer (PBS with 1% FCS and 0.1% NaN_3). After the cells were washed twice, they were fixed and permeabilized by using a Cytofix/Cytoperm kit (BD Biosciences) and stained with a fluorescein isothiocyanate (FITC)-conjugated rat antimouse IFN-γ mAb (clone XMG1.2; BD Biosciences). After the cells were washed, flow cytometric analyses were performed with a FACScanto II flow cytometer (Becton Dickinson, Franklin Lakes, NJ, USA), and the data were analyzed with FACSdiva software (Becton Dickinson).

PD-1 and Tim-3 staining

Intrahepatic lymphocytes were prepared and treated with an antimouse CD16/CD32 mAb as described above for intracellular IFN-γ staining and then stained with a PE-conjugated HCV-NS3 H-2Db tetramer, PerCP-conjugated anti-CD8a (BD Biosciences), FITC-conjugated anti-PD-1 (eBioscience, San Diego, CA, USA) and Alexa647-conjugated anti-Tim-3 (Biolegend, San Diego, CA, USA) for 30 min at 4°C. After the cells were washed twice, they were fixed with PBS containing 1% formaldehyde and 2% FCS and analyzed by flow cytometry.

PD-L1 staining

Intrahepatic APC were prepared and treated with an antimouse CD16/CD32 mAb as described above for intracellular IFN-γ staining and then stained with a FITC-conjugated anti-CD11c (BD Biosciences) and PE-conjugated anti-PD-L1 (eBioscience) for 30 min at 4°C. After the cells were washed twice, they were fixed with PBS containing 1% formaldehyde and 2% FCS and analyzed by flow cytometry.

HCV core Ag detection

For the detection of HCV core Ag in the liver, liver tissue samples isolated 7 and 14 days post-infection were homogenized in RIPA B buffer (50 mM Tris pH 7.5, 1% NP40, 0.15 M NaCl, 1 mM phenylmethylsulfonyl fluoride) to make 10% (w/v) extract. Liver tissue extracts were assessed using Lumispot Eiken HCV Ag assay kit (Lumispot-Ag; Eiken Chemical, Tokyo, Japan).

Histology and immunohistology staining

Liver tissue samples isolated 7 and 14 days post-infection were used for histological studies. Paraffin sections (4-μm thick) were stained with hematoxylin–eosin safranin O. For immunohistology, 5-μm thick acetone-fixed frozen sections were incubated with rat anti-CD8 (BD Biosciences), followed by biotin-conjugated antirat immunoglobulin G and ABC staining system (Santa Cruz Biotechnology, Santa Cruz, CA, USA).

Persisting HCV-NS3 Ag detection

For the detection of persisting HCV-NS3 Ag in the liver, liver tissue samples isolated 21 days post-infection were homogenized in RIPA C buffer (50 mM Tris pH 7.5, 1% Triton X-100, 300 mM NaCl, 5 mM ethylenediaminetetraacetic acid, 0.02% NaN_3) to make 2% (w/v) extract and used for immune precipitation/western blot assay. Liver tissue extracts were incubated with protein-G sepharose beads for 30 min at 4°C to remove non-specifically bound proteins. After centrifugation, supernatants were incubated with anti-Flag-M2 antibody (Sigma-Aldrich) coupled protein-G sepharose beads for 2 h at 4°C. After centrifugation, HCV-NS3-3xFlag fusion protein bound to the beads were dissolved in sample buffer and separated on 10% sodium dodecylsulfate polyacrylamide gel electrophoresis gels (Mini PROTEAN TGX gel; Bio-Rad, Hercules, CA, USA) for immunoblot analysis using anti-Flag-M2 antibody and goat anti-mouse Ig horseradish peroxidase (KPL, Gaithersburg, MD, USA). Electrochemiluminescence Prime Western Blotting Detection Reagent (GE Healthcare, Little Chalfont, UK) was used for chemiluminescent detection.

Statistical analysis

Mann–Whitney *U*-tests were used to evaluate the significance of the differences. Correlations between parameters were tested for statistical significance by Pearson correlation.

RESULTS

Functional exhaustion of Ag-specific CD8 IHL with high infectious dose and the impaired Ag-specific CD8 IHL responses in core Tg mice

TO DETERMINE THE effect of the amount of virus dose, we evaluated hepatic inflammation and compared the magnitude of HCV-NS3-specific CD8

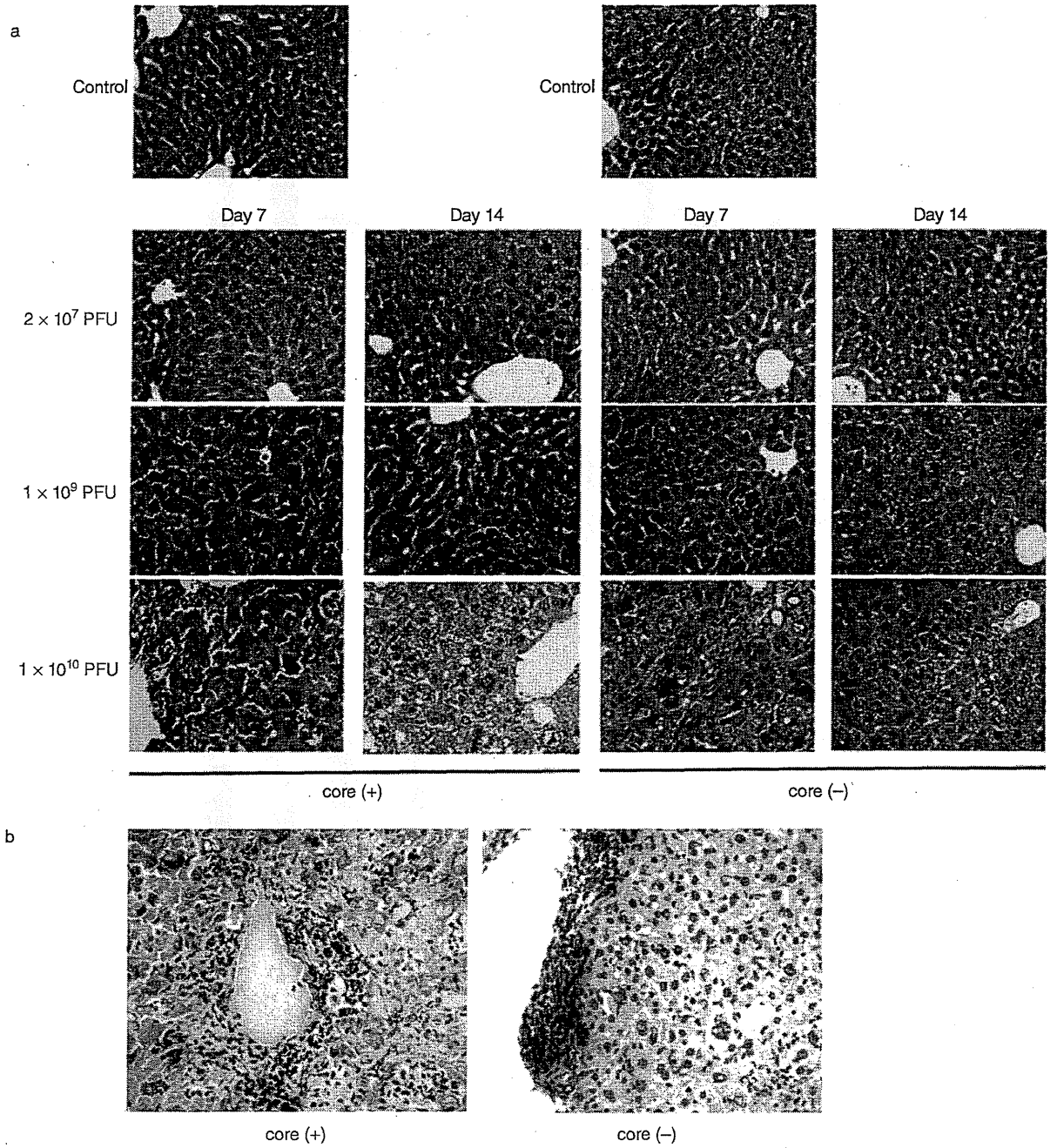

Figure 1 Adenovirus (Ad) infection-mediated hepatic inflammation in mouse liver. Hepatitis C virus (HCV) core (+) and core (–) mice were infected with 2×10^7, 1×10^9 and 1×10^{10} plaque-forming units (PFU) of Ad-HCV-NS3 i.v. and analyzed at 7 and 14 days post-infection. (a) Harvested liver tissues were analyzed by hematoxylin–eosin staining for assessment of hepatic inflammation. (b) Frozen liver sections were analyzed by CD8 staining. Liver infected with 1×10^{10} PFU and harvested at 7 days post-infection was used (original magnifications: [a] ×100; [b] ×200). (c,d) The frequency and number of hepatic CD8 lymphocytes were assessed by flow cytometric analysis. There were no differences in the frequency and number of hepatic CD8 lymphocytes between core (+) mice and core (–) mice. (e) Detection of HCV core antigen in the liver. Liver tissue extracts were assessed using Lumispot Eiken HCV Ag assay kit. There were no differences in core protein expression between Ad-infected and non-infected livers. ■, day 7; ▩, day 14; □, day 21.

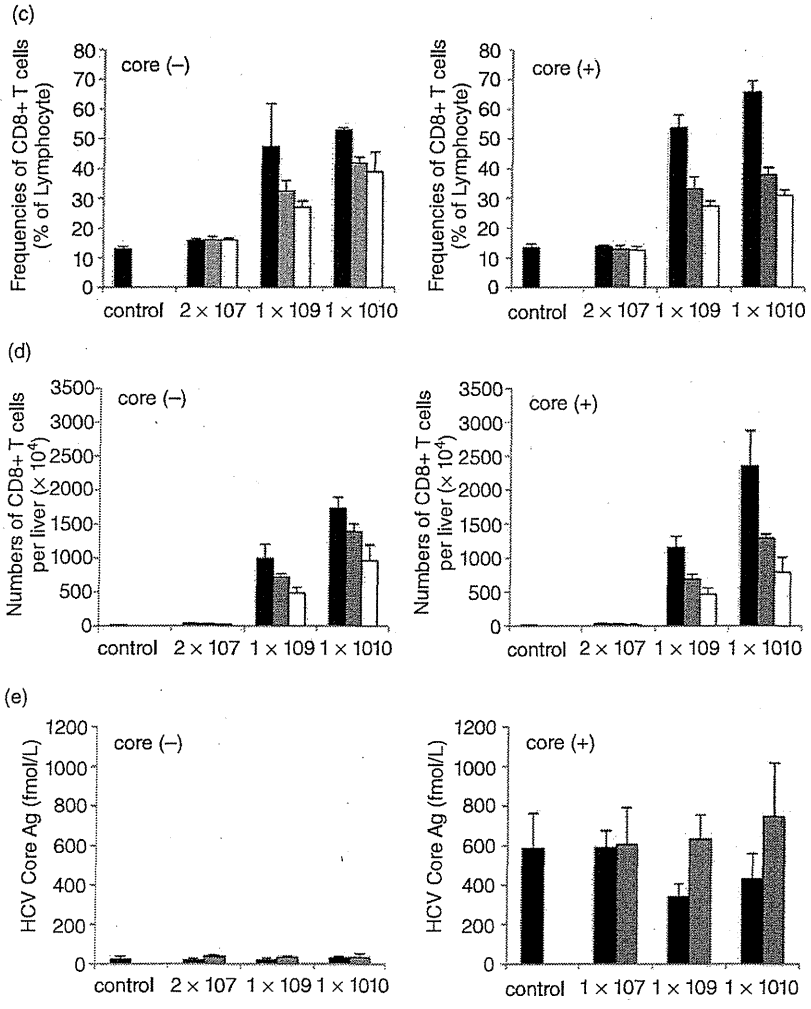

Figure 1 *Continued*

T-cell responses and their effector function in the liver of mice infected with 2×10^7, 1×10^9 and 1×10^{10} PFU Ad-HCV-NS3.

In histological studies, we observed Ad-infection-mediated hepatic inflammation in mice injected with 1×10^9 and 1×10^{10} PFU. Especially, infection with 1×10^{10} PFU caused drastic infiltrations of inflammatory cells (Fig. 1a). We also observed that CD8 lymphocytes infiltrated into the lobular areas of the infected liver in mice injected with 1×10^{10} PFU (Fig. 1b). At 7 days post-infection, we found by flow cytometric assay that the numbers and the frequencies of CD8 T cells in the liver were markedly increased after infection with 1×10^9 PFU and 1×10^{10} PFU, and the increased CD8 T cells decreased with time (Fig. 1c). We did not find significant differences between the number of CD8 T cells of core (+) and core (–) at each time point and infectious dose.

In addition, we evaluated core protein expression in the liver in each infectious dose at 7 and 14 days post-infection; there was no significant difference in core protein expression between Ad-infected and non-infected livers (Fig. 1e).

Using major histocompatibility complex (MHC) class I tetramer complexed with the H2-Db-binding HCV-NS3 GAVQNEVTL epitope, we found that i.v. infection with 2×10^7 PFU generally elicited only a weak expansion of HCV-NS3 tet$^+$ CD8$^+$ IHL (Fig. 2a,b) and IFN-γ^+ HCV-NS3 tet$^+$ CD8$^+$ IHL (Fig. 2a,c). In contrast, infection with 1×10^9 PFU induced a significant proliferation

of HCV-NS3 tet$^+$ CD8$^+$ IHL (Fig. 2a,b) and IFN-γ$^+$ HCV-NS3 tet$^+$ CD8$^+$ IHL (Fig. 2a,c).

In each infectious dose, HCV-NS3 tet$^-$ CD8 IHL did not show the diminution of elicited IFN-γ production (Fig. 2a). In contrast, HCV-NS3 tet$^+$ CD8 IHL showed the dose-dependent diminution of elicited IFN-γ production (Fig. 2d). Especially, infection with 1×10^{10} PFU led to a dramatic diminution of the elicited IFN-γ production in HCV-NS3 tet$^+$ CD8$^+$ IHL (Fig. 2a,d). These indicate that high infectious dose of Ad-HCV-NS3 cause NS3 Ag-specific immunosuppression.

As shown in Figure 2(c), the number of IFN-γ-producing HCV-NS3 tetramer$^+$ CD8 T cells in the liver of core (+) mice was lower than that of core (−) mice following PMA/ionophore stimulation. In addition, the percentage of IFN-γ-producing CD8 lymphocytes in tetramer$^+$ CD8 IHL of core (+) mice was suppressed as compared with core (−) mice following PMA/ionophore stimulation (Fig. 2d). These suggest that the presence of HCV core gene significantly impair antiviral effector CD8 T-cell responses in the liver.

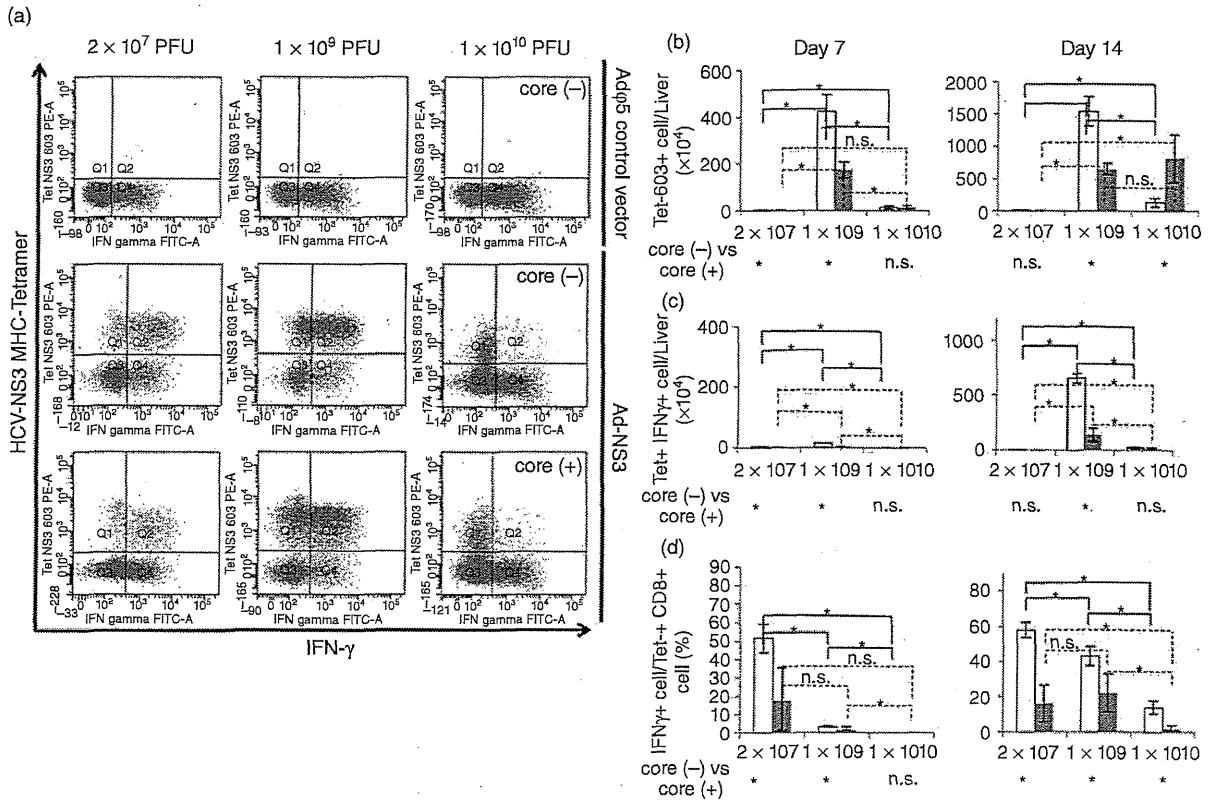

Figure 2 Impaired CD8$^+$ T-cell responses in the livers of high infectious doses. (a) Flow cytometric dot gram gating on the CD8 lymphocyte at day 14 post-infection. Graded doses of adenovirus (Ad)-hepatitis C virus (HCV)-NS3 were administrated i.v and NS3-specific intrahepatic cytotoxic T lymphocytes (CTL) were analyzed using major histocompatibility complex (MHC) class I tetramer and intracellular interferon (IFN)-γ staining method. Data show one representative mouse per group ($n = 3$). (b) The number of MHC tetramer$^+$ CD8 lymphocytes in the liver of core (−) and core (+) mice at day 7 and day 14 following Ad-HCV-NS3 infection (*$P < 0.05$; n.s., not statistically significant). (c) The number of tetramer+ intracellular IFN-γ + CD8 lymphocytes in the liver of core (−) and core (+) mice at day 7 and day 14 following Ad-HCV-NS3 infection. Intrahepatic lymphocytes (IHL) were restimulated with phorbol myristate acetate (PMA)/ionophore for 5 h and IFN-γ production was determined by intracellular cytokine staining (*$P < 0.05$; n.s., not statistically significant). (d) The percentage of intracellular IFN-γ$^+$ CD8 lymphocytes in tetramer$^+$ CD8 IHL of core (−) and core (+) mice on day 7 and day 14 following Ad-HCV-NS3 infection. IHL were restimulated with PMA/ionophore for 5 h and IFN-γ production was determined by intracellular cytokine staining (*$P < 0.05$; n.s., not statistically significant). □, core (−); ▩, core (+).